BIOSYNTHESIS OF PRION PROTEIN NUCLEOCYTOPLASMIC ISOFORMS BY ALTERNATIVE INITIATION OF TRANSLATION

María E. Juanes[1], Gema Elvira[1], Aranzazu García-Grande[2], Miguel Calero[3], and María Gasset[1]*

[1]Insto Química-Física "Rocasolano", CSIC, Serrano 119, 28006 Madrid, Spain; [2]Centro Nacional de Investigaciones Oncológicas, Melchor Fernández Almagro 3, 28029 Madrid, Spain. [3]Centro Nacional de Microbiología, Insto. Salud Carlos III, Ctra. Pozuelo Km 2, 28220 Majadahonda, Madrid, Spain

Running head: **Nucleocytoplasmic PrP isoforms**

***Address correspondence to: María Gasset, Insto Química-Física "Rocasolano", CSIC, Serrano 119, 28006 Madrid, Spain; Tel: +34915619400, Fax: +34915612431, E-mail: mgasset@iqfr.csic.es

The cellular prion protein PrP^C is synthesized as a family of four distinct forms. Of these, ^{Cyt}PrP is a minor member that segregates outside of the secretory route and can generate cytotoxic forms. Using signal sequence mutants, we found that ^{Cyt}PrP is translated from a downstream AUG (coding for M8 in HuPrP or M15 in HaPrP). Shortening of the signal sequence dictated the spillage of this isoforms into the cytosol, from where it accessed the nucleus or formed insoluble cytosolic aggregates if the proteasome is inhibited. The PrP isoform isolated from the nuclear fractions of cell and brain homogenates was partially SUMO-1 conjugated. Expression of HaPrP(M15) in cells caused an anti-proliferative phenotype due to a cell cycle arrest at the G_0/G_1 phase. The identification of this PrP isoform and its properties provides novel insight into PrP^C physiological and pathological functions.

The cellular prion protein (PrP^C) underlies a group of fatal neurodegenerative diseases through its conversion into self-perpetuating and neurotoxic forms [1-4]. Despite a large amount of evidence supporting a role in survival-death and growth-differentiation cell decisions, the physiological function of PrP^C and its involvement in disease remain elusive [5-8]. A crucial limiting factor for PrP^C functional determination is its molecular diversity. Although PrP^C is mainly thought of as a glycoprotein attached to the cell surface by a glycosylphosphatidylinositol anchor, PrP^C is actually synthesized as a family of four members: the membrane anchored glycoprotein (^{Sec}PrP), two transmembrane forms with opposite topologies (^{Ntm}PrP and ^{Ctm}PrP) and a soluble form (^{Cyt}PrP) [3, 9-12].

Of these different members, ^{Cyt}PrP accounts for a minor intracellular subset of PrP^C that has attracted much attention because its accumulation sensitizes cells to death [13-15]. Initially, ^{Cyt}PrP was thought to be formed by misfolded chains that retrotranslocated through the endoplasmic reticulum-associated protein degradation-proteasome pathway [16,17]. However, it was later shown that ^{Cyt}PrP is constitutively populated by nascent chains that spill into the cytosol due to inefficient N-terminal signalling [15,18]. Regarding the role of ^{Cyt}PrP, most knowledge has been provided by models consisting of mutant polypeptide chains that are inappropriately expressed and folded in the cytosol. These PrP(23-230) chains exhibit a widespread intracellular distribution [19-21] and an allegedly role that varies from cytotoxic [14,20] to innocuous or even protective [19,22,23]. These contradictions call into question the fidelity with which such models can describe ^{Cyt}PrP.

The finding that information for ^{Cyt}PrP synthesis is contained in its N-terminal signal sequence [15] prompted us to decipher this code and use it as a tool to isolate its synthesis from that of the major forms and inspect its function. We have found that ^{Cyt}PrP is indeed a novel PrP isoform that access the nucleus and interferes with cell growth. These results provide new insights on PrP diversity and its role in health and disease.

EXPERIMENTAL PROCEDURES

Plasmid construction and recombinant standard production. The plasmid pcDNA4-HaPrP, kindly provided by Dr. RS Hegde, was first mutated to introduce the 6 nucleotides from the 5´-UTR region adjacent to the initial ATG in order to preserve the wild type Kozak sequence. HuPrP ORF was cloned into pcDNA3.1 at *BamHI*/*EcoRI* sites preserving the corresponding

wild type Kozak region. Wild-type constructs were used as templates to generate different mutants (Table 1, Figure 1) by using Quickchange protocols (Stratagene). The integrity of each construct was verified by sequencing. Recombinant PrP chains (rPrP) of 1-254, 15-231, 15-254 and 23-231 were produced from the corresponding pET11a plasmids in *E.coli* BL21(DE3) and used as inclusion bodies denatured extracts as previously described [5].

Transcription, translation and translocation assays. All plasmids were enzymatically linearized (pcDNA4.1-HaPrP plasmids with *ApaI* and pcDNA3.1-HuPrP constructs with *SacII*) and then transcribed with the T7 CapScribe kit (Promega). After integrity verification, the transcribed mRNAs were translated at 80 μg/ml final concentration using 50% (v/v) nuclease-treated rabbit reticulocyte lysate system (Promega) and Redivue™ L-[^{35}S]methionine (Amersham Biosciences), as indicated by the manufacturer. For translation-translocation assays, the reaction mixture was enriched in 15% (v/v) canine pancreatic rough microsomal membranes [24, and references therein]. Isolation of the fraction of sealed microsomes from the reaction mixtures was performed by discontinuous sucrose gradient ultracentrifugation as previously described [24]. For protease protection analysis, the total reaction mixtures and their sealed microsomal fractions were incubated for 1 h at 4°C with 0.1 mg/ml proteinase K (Roche Diagnostics) both in the absence and presence of 0.5 % Triton X-100. The reaction was stopped with 5 mM PMSF. The ^{35}S-labeled reaction products were immunoprecipitated with αPrP 3F4 mAb (Signet Lab), resolved on Tris-Tricine 16.5% PAGE-SDS gels and visualized using a PhosphorImager (Fuji Fla 3000). Enzymatic deglycosylation was performed by incubating the immunoprecipitated samples with PNGase F (New England BioLabs) according to the manufacturer´s instructions.

Cell culture, transfections and treatments. CHO and COS-7 cells were grown and maintained in DMEM supplemented with 10% fetal bovine serum, 2 mM glutamine, 10 IU/ml penicillin, and 10 μg/ml streptomycin in a humidified atmosphere of 5% CO_2 at 37°C. Transfection of cells with the different plasmids was performed with TransIT-LT1 (Mirus) following the manufacturer´s indications. After 48 h, cells were processed for analysis or used for bulk selection of stable transfectants. For proteasome impairment experiments, 24 h after transfection cells were treated in the absence or presence of 5 μM MG132 for 18 h [15]. Alternatively, after 4h the medium was changed and the incubation was continued for another 14h [15]. After PBS washes, cells were harvested and analyzed for protein aggregation (see below).

Cell lysates, brain homogenates and fractionations. Denatured cell lysates were prepared at about 15 mg/ml protein concentration in 62.5 mM Tris-HCl pH 6.8 containing 4% SDS (w/v) and 25% glycerol (w/v), boiled for 10 min and then cleared by centrifugation at 15000xg for 20 min. Hamster brains were obtained from the Animal Facility of the Instituto de Investigaciones Biomédicas "Alberto Sols" UAM-CSIC. Human cortex control samples were obtained from the Institute of Neuropathology and University of Barcelona/Clinic Hospital brain banks following the guidelines of the local ethics committees. Tissue homogenates at 10% (w/v) were prepared in PBS pH 7.5, containing 0.25 M sucrose, 1.5 mM sodium orthovanadate, 5 mM EDTA and the EDTA-free Complete protein inhibitor cocktail (Roche Diagnostics), aliquoted and kept at -80 °C. Fractionation of cell and tissue homogenates into nuclear and post-nuclear fractions was performed using the Pure Prep Nuclei isolation kit (Sigma) following the manufacturer indications. The final step including PIPLC digestion was introduced to ensure the removal of contaminant raft-resident PrP^C.

Protein aggregation assays. Analysis of PrP aggregation upon proteasome inhibition was performed with minor modifications to published methods [13, 15-17]. Cells were lysed in cold EZ-lysis buffer and then separated into pellet (nuclear) and supernatant (post-nuclear) fractions by a 500xg centrifugation for 10 min at 4 °C. The pellets were washed twice with EZ-lysis buffer for isolation of the nuclear fractions. The post-nuclear supernatants were supplemented with 0.5% Triton X-100 and 0.5% deoxycholate, dispersed by extensive pipetting and then centrifuged for 10 min at 13,000xg at 4°C. Proteins in the supernatant were precipitated with cold 15%TCA. All protein pellets were resuspended in 0.1M Tris-HCl pH 8.0, 1% SDS and equal aliquots of each fraction were analyzed by SDS-PAGE and immunoblotting.

Immunoprecipitation and western blotting. Samples were lysed in 62.5 mM Tris-HCl pH 6.8 containing 4 % (w/v) SDS and 25 % (w/v) glycerol. After a 10 min spin at 10000xg, the supernatants were diluted 1:40 with PBS pH 7.4 containing 0.1% sodium deoxycholate

(Calbiochem), 1% NP-40 (Sigma-Aldrich), 1.5 mM sodium orthovanadate and 1 mM PMSF. Samples were incubated for 1 h with Protein A/G-Sepharose (Amersham Biosc.). After a 5 min centrifugation at 200xg, the supernatants were incubated with either 3F4 or SP α-PrP antibodies at 4 ^{o}C and the resulting immunocomplexes were captured with Protein A/G-Sepharose and released using Laemmli buffer. Proteins (~50 μg per lane) were separated by electrophoresis on 13 % SDS-polyacrylamide gels and blotted onto PVDF membranes (150 V, 1 h). The membrane-bound proteins were probed with the primary antibody followed by mouse True-blot HRP conjugated α-mouse IgG (1:1000, eBiosciences), goat α-mouse HRP-conjugated IgG (1:3000, Sigma) or goat α-rabbit HRP-conjugated IgG (1:8000, Chemicon), and then developed with chemiluminescent Chemicon reagents. Data acquisition and analysis were carried out using the Bio-Rad ChemiDoc equipment. The following primary antibodies and dilutions were used: αPrP 3F4 (1:5000, Signet Lab), αPrP α-SP (1:1000, provided by D. Harris and raised against PrP N-terminal signal peptide), α-YFP (1:3000, α-GFP Abcam), α-PDI (1:1000, Abcam), α-βCOP (1:1000, Abcam), α-Histone H3 (1:2000, Abcam); α-ubiquitin P4D1 (1:200, Santa Cruz Biotech), α-SUMO-1 D-11 (1:200, Santa Cruz Biotech), and β-actin (1:5000, Sigma-Aldrich).

Confocal fluorescence microscopy. Cells were plated onto glass coverslips, allowed to attach for 24 h and then transfected for 48 h. Cells were fixed with 4% paraformaldehyde in PBS containing 5% sucrose for 10 min at room temperature and washed three times with PBS. Cells were permeabilized and blocked in PBS containing 0.5% saponin, 0.1% Triton and 2% bovine serum albumin for 10 min at room temperature. Cells were incubated with αPrP 3F4 (1:600) and with α-PDI (1:600) for 1 h at room temperature. After three washes with blocking buffer, samples were incubated with Alexa-647-conjugated goat α-mouse IgG (1:800), Alexa-488-conjugated α-rabbit IgG (1:800), and Hoechst 33342 (10 μg/ml) in blocking solution for 30 min at room temperature. After washing, the coverslips were mounted on glass slides with ProLong Gold antifade reagent (Molecular Probes). Images were captured with a confocal microscope (Leica TCS-SP-AOBS-UV) using the UV and Ar lasers at 20 mW for excitations at 364 nm (Hoescht) and 488 nm (Alexa-488), respectively, and the 633 nm line of the He-Ne laser at 10 mW for excitation at 647 nm. Image analysis was performed using Leica confocal software.

Cell proliferation assays and cell cycle analysis. For cell growth analysis, cells were co-transfected with pEYFP (Clontech) and the plasmid coding wild type HaPrP or its mutants. After 48 h of transfection, cells were synchronized in G_0/G_1 by serum deprivation for 18 hours and then released by serum supplementation for 6 h. Cell proliferation was analyzed in 96-well format using the BrdU cell proliferation kit (Calbiochem) and a MR500 microplate reader (Dynatech). BrdU labeling was performed for 6h during the 10% FBS stimulation period. Cell cycle profiles were determined by flow cytometry using the standard measurement of DNA content with propidium iodide (PI) in a BD FACS-Calibur cytometer (BD Biosciences). In this case, YFP-positive cells were selected by cell sorting before PI labelling. Data were compared by one- or two-way ANOVA with Bonferroni´s post-test analysis using GraphPad Prism v 4.0.

RESULTS

N-terminal signal peptides of PrP contain a dual methionine motif. N-terminal signal peptides display a tripartite organization into n-, h- and c-regions, with the hydrophobic central region (h-region) essential for co-translation membrane integration and translocation process. The signal sequences of PrP from different species can be classified into three groups on the basis of the number of M residues and their position with respect to regional boundaries (Figure 1). Group I, represented by the rodent sequences, contains two M residues at positions 1 and 15; the second position is in the N-terminal side of the c-region. In Group II, represented by the human sequence, the two M residues are at positions 1 and 8. In this case the second M constitutes the N-terminus of the h-region. On the contrary, Group III, which is represented by the mink sequence, lacks of the second M residue. When converted into their cognate mRNA sequences, the M residues of the signal sequences become AUG codons that could behave as translation initiation sites. We also identified two in-frame triplets (CUG and GUG coding HaPrP L9 and V13) that could sustain translation initiation by means of a single base difference. These non-AUG codons are conserved in all species. If used, any of these codons could yield nascent chains with different cellular fates.

The MM motif allows a dual translation start and the existence of PrP isoforms. To test whether the downstream AUG codons found in the signal sequence regions of PrP mRNA in group I and group II could sustain translation initiation, we generated a series of point mutations in both the HaPrP and HuPrP ORFs [Figure 1, 2 and Table 1]. These mutations consisted of the insertion of a C or a G at various positions causing a +1 shift in the reading frame (11C12, 13G14, 16C17), as well as an M-to-S substitution (ATG-to-TTC). The reading frame shift mutations allow the study of both non-AUG and AUG start sites, whereas the M-to-S substitutions permit the evaluation of the role of a specific M residue. It should be noted that frame shift mutations allow translation initiation at either start sites but only the product produced from the start site downstream from the insertion will proceed to the wild type (wt) stop codon and will produce chains retaining the 3F4 PrP epitope.

The results of the translation of the mRNAs coding for wt and mutant HaPrP and HuPrP using reticulocyte lysates followed by immunoprecipitation with 3F4 are shown in Figure 2A. In agreement with previous reports, wild type HaPrP mRNA was translated into a major polypeptide chain of about 26 kDa. Under the same conditions, translation of the mRNA coding HaPrP(M1S), in which the canonical AUG is functionally impaired, and for the reading frame shift mutants HaPrP(11C12) and HaPrP(13G14) led to the production of a single product of similar mass (26 kDa), but with reduced intensity (about 10-15% of that of the wt). On the contrary, translation of the mRNAs coding HaPrP(16C17) and HaPrP(M1S,M15S) resulted in the absence of any detectable signal. These results support the idea that HaPrP mRNA contains a minor translation initiation site and that this site is located at codon 15, the AUG triplet coding for M15. It should be noted that the chains translated from M1 and M15 could not be easily differentiated by electrophoresis probably as a result of the balance between the differences in size and hydrophobicity of the chains [25].

The translation of wt HuPrP mRNA yielded a band corresponding to a polypeptide chain of about 27 kDa [Figure 2A]. This band was detected using the mRNAs of the HuPrP(M1S) and HuPrP(5T6) mutants, but with less intensity. On the contrary, this band was not observed using the mRNAs of the HuPrP(11T12), HuPrP(13T14), HuPrP(16T17) and HuPrP(M1S,M8S) mutants. These results show that HuPrP mRNA, as model for group II, also contains a minor translation start site and that this site is located at codon 8, the AUG triplet coding for M8.

Since the alternative translation start site of PrP signal sequences in groups I and II is due to the dual methionine motif, it follows that the sequences of Group III either lack this capacity or utilize a different process.

HaPrP(M15) and HuPrP(M8) isoforms account for *de novo* synthesized ^{Cyt}PrP. To unambiguously establish the relationship between HaPrP(M15) and HuPrP(M8) and *de novo* synthesized ^{Cyt}PrP, we studied their behavior in cell-free biosynthesis assays [Figure 2B, 2C]. Figure 2B shows that in contrast to the wt mRNAs, the products of mRNAs coding HaPrP(M1S) and HuPrP(M1S) mutants and translated in the presence of microsomal membranes consisted of a single band of ~26 kDa that remained unchanged after PNGase F digestion. Comparison of the bands after deglycosilation, in particular of HuPrP chains, suggests that HuPrP(M1S) migrates similarly to an unprocessed full length chain (see below) [26]. The unglycosylated pattern agrees with a cytosolic location for the HaPrP(M15) and HuPrP(M8) C-terminal domains. Furthermore, external addition of proteinase K to both the total reaction mixture and its sealed microsome fraction (no signal was detected in this fraction even using at a 10x overload compared to the wt) resulted in complete degradation of the ~26 kDa chains translated from the HaPrP(M15) and HuPrP(M8) mRNAs [Figure 2C]. In contrast the product translated from wt mRNAs under similar conditions showed protected fragments corresponding to translocated and integrated PrP chains [3]. Taken together, these results suggest that HaPrP(M15) and HuPrP(M8) chains segregate outside the secretory route under a proteinase K-sensitive conformation as described for ^{Cyt}PrP.

To determine whether the synthesis of these isoforms takes place in cellular contexts, we proceeded with transient transfection experiments using CHO and COS-7 cells, which have undetectable levels of endogenous PrP expression. In this case, the study was restricted to the HaPrP sequences for biosafety reasons and was performed as co-transfection with pEYFP in order to use YFP expression as an internal control. Plasmids encoding HaPrP wt and HaPrP(M1SM15S) were used as positive and negative controls for PrP^{C} expression, respectively, whereas those encoding HaPrP(11C12) and HaPrP(M1S) were employed to assess the functionality of M15 as start site. Figure 3A shows that HaPrP(M15) was indeed synthesized by cells based on the presence of a 26 kDa band recognized by αPrP 3F4 in the lysates

of HaPrP(11C12) and HaPrP(M1S) transfectants. Importantly, the 26 kDa band was also recognized by α-SP, an antibody raised against the C-terminal region of the signal sequence [11]. In cell lysates HaPrP(M15) retained the C-terminal hydrophobic segment according to electrophoretic mobility determinations using a panel of recombinant PrP chains consisting in the full unprocessed chain (1-254 sequence), fully processed chain (23-231 sequence) and N-terminally shortened chains either containing (15-254) or lacking (15-231) the C-terminal hydrophobic segment [Figure 3B].

To corroborate that the HaPrP(M15) synthesized in cells behaves as ^{Cyt}PrP, we studied its glycosylation state as well as its capacity to form insoluble aggregates upon proteasome impairment [13, 15-17]. Figure 3C shows that in contrast to wt HaPrP, 26 kDa HaPrP(M1S) remained unchanged upon PNGase F digestion as expected for ^{Cyt}PrP. Moreover, both transient and irreversible inhibition of the proteasome with 5 μM MG132 promoted the formation in the cytosol of insoluble HaPrP(M1S) aggregates [Figure 3D]. Both the absence of glycosylation and the capacity to form cytosolic insoluble aggregates confirms that HaPrP(M15) behaves as ^{Cyt}PrP in a cellular context.

HaPrP(M15) and HuPrP(M8) are found in nuclei isolated from cells and normal brain homogenates, and are sumoylated. To elucidate the properties of these isoforms, we first studied their subcellular location using confocal microscopy. Unless stated, HaPrP(M15) was expressed from the HaPrP(Δ14) construct for easier detection. Indirect immunofluorescence stainings showed that at 48 h after transfection, HaPrP(M15) was localized largely to the nuclei of cells [Figure 4A]. The distribution pattern agreed with the diffuse nucleoplasmic location observed for several studied ^{Cyt}PrP models [19, 27], and differed from the intranuclear granules observed in neuronal cells expressing BoPrP^{C} [28]. The nuclear localization was then confirmed by subcellular fractionation of cell homogenates. Figure 4B shows that about 70% of the expressed HaPrP(Δ14) was localized to the nuclear fraction, mainly as a 26 kDa chain but also as higher molecular weight species. Similar results were obtained using CHO and COS-7 cells.

To generalize the nuclear localization of HaPrP(M15), as well as to determine the origin of the high molecular weight bands, we purified the nuclei from normal hamster brain and human cortex homogenates and characterized the PrP contained therein. Before the analysis the purified nuclei were dispersed in EZ-lysis buffer, digested with PIPLC and then centrifuged at low speed. This process allows the release of the contaminant membrane-anchored forms [29], Figure 5A shows that after removing raft-resident PrP^{C}, PrP was detected in the nuclei purified from hamster brain homogenates as two bands of 26 and 35 kDa that remained unchanged after enzymatic deglycosylation. Nuclear PrP in human cortex was also comprised of two major PNGaseF-resistant bands of about 26 and 35 kDa. These bands were recognized by both 3F4 and α-SP, as expected from PrP chains bearing N-terminal shortened signal peptides [Figure 5B]. These data confirm the existence and nuclear distribution of isoforms produced by alternative translation in normal tissues.

The complexity of the bands suggests the occurrence of covalent modifications. Of the modifications that can occur in nuclear proteins and cause increases in size, activity-modifying sumoylation and degradation-targeting ubiquitinylation were studied. Figure 5C shows that high molecular weight bands of PrP immunoprecipitated with 3F4 from denatured nuclei extracts of hamster brain homogenates were recognized by an anti-SUMO-1 antibody but not by anti-ubiquitin or anti-SUMO 2/3 antibodies. Inverse pull-down experiments with α-SUMO-I confirmed 3F4 immunorreactivity. Since SUMO-1 conjugation involves the covalent attachment of a single 9.5 kDa chain, the observed band pattern can be explained to large extent by considering the composition of a non-sumoylated chain (26 kDa) and a SUMO-I conjugated form (35 kDa).

In summary, PrP(M8/M15) appear to be a nuclear isoform that acts as substrate for SUMO-1 conjugation.

HaPrP(M15) expression abrogates cell proliferation. Trials to establish cell lines expressing HaPrP(M15) were unsuccessful despite the absence of a conclusive and reproducible cell death event. Stably transfected clones were selected, but they failed to grow. These growth alterations together with the nuclear distribution and involvement of reversible sumoylation prompted us to consider a possible anti-proliferative activity.

Analysis of BrdU incorporation showed that HaPrP(M15) did indeed decrease cell growth as compared to HaPrP wt and the negative control HaPrP(M1SM15S) in both COS-7 and CHO cells [Figure 6A]. This effect was more pronounced and statistically significantly higher ($p<0.001$) for the HaPrP(Δ14) mutant, which overexpresses the PrP isoform [Figure 3A], than the HaPrP(M1S) and HaPrP(11C12) mutants.

The cell cycle was then analyzed using a co-transfection approach. In this case cells were co-transfected with pEYFP for separation of the positive transfectants by cell sorting before PI labeling. Figure 6 [panels B and C] shows that cells expressing HaPrP(M15) from both HaPrP(Δ14) and HaPrP(11C12) constructs exhibited a higher proportion of cells in the G_0/G_1 phase as compared to the mock control [transfection with HaPrP(M1SM15S)]. These results indicate that HaPrP(M15) functions as a growth suppressor that delays the exit from G1 phase.

DISCUSSION

In this study we have shown that the minor member of the PrP^C family segregating outside the secretory route is generated by alternative initiation of translation. The presence of a second M residue at the h-region boundary of the signal sequence determines the alternative translation initiation event. This process permits the synthesis of an isoform translated from either M15 in HaPrP or from M8 in HuPrP. This isoform represents a novel chain differing from the conventional mature form in the retention of the c-region of the N-terminal signal sequence and the full C-terminal hydrophobic region. These two segments could provide new functions as stability regulators or as sites of interaction for distinct ligands, among others.

The use of in-frame alternative translation start sites is a relatively common process by which proteins encoded by a single mRNA can acquire multiplicity of sorting and function under environmental regulation [30-34]. Although the relative proportion of PrP(M15) synthesis was about 12% both in the *in vitro* studies and cell systems used for transfection, it might be susceptible to such modulation. This is supported by the cell- and regional dependency of ^{Cyt}PrP in normal rodent brains as well as its increased levels under ER stress [23,35]. As noted the dual start site motif is missing in a group of highly conserved PrP sequences. In these sequences the AUG triplet coding for M15 is found as either ACG or ACA, which code for T. Of these two codons, ACG can function as a non-AUG start site [36,37]. However, the function of the ACA triplet as a start is unclear, thus whether ACA-bearing species use the alternative translation mechanism remains to be established.

Isolating the synthesis of HaPrP(M15) from that of the major membrane-bound PrP forms allowed three major findings: nuclear localization, variable SUMO-1 conjugation, and anti-proliferative activity. The nuclear localization of this isoform might explain results of previous PrP studies describing rare nuclear localization, the presence of NLS, and the capacity of the chain to interact with nucleic acids and with chromatin [19, 28, 38].

SUMO-1 conjugation of the nuclear population of PrP suggests stringent regulation of activity and physiological relevance for this isoform. In general, sumoylation provides an on/off functional switch for protein interactions involved in processes such as transport, transcriptional silencing, genomic stabilization and stress responses [39]. SUMO-1 conjugated and free HaPrP(M15) chains might thus represent alternative functional states of the molecule. It is thus interesting to note that the degree of sumoylation in nuclei from brains was higher than that in cells. With the limitations imposed by the lack of sumoylation control, HaPrP(M15) expression might be involved in dysregulation of cellular growth resulting in G_0/G_1 phase arrest.

The anti-proliferative function of HaPrP(M15) expands the physiological role of PrP^C. Since most cells withdraw from the cell cycle in order to differentiate during the G1 phase, it is tempting to consider HaPrP(M15) as candidate for promotion of G1-phase arrest required for cell differentiation in some developing tissues [7]. On the other hand, the loss of HaPrP(M15) nuclear functionality might favor either cell transformation on depletion [8] or cell death on cytosolic accumulation [15]. HaPrP(M15) can regulate the efficiency of prion accumulation, which decreases with cell division [40].

The isolation of the synthesis of this isoform from that of other members of the PrP^C family suggests that each member of this family might have different physiological roles and that their aberrant cross-talk could also constitute a pathogenic mechanism.

REFERENCES

1. Aguzzi, A., and Polymenidou, M. (2004) *Cell* **116**, 313-327
2. Gasset, M., Baldwin, M.A., Lloyd, D.H., Gabriel, J.M., Holtzman, D.M., Cohen, F., Fletterick, R., and Prusiner, S.B. (1992) *Proc Natl Acad Sci U S A.* **89**, 10940-10944.
3. Hegde, R.S., Mastrianni, J.A. , Scott, M.R, DeFea, K.A., Tremblay, P., Torchia, M., DeArmond, S.J., Prusiner, S.B., and Lingappa, V.R.. (1998) *Science* **279**, 827-834.
5. González-Iglesias, R., Pajares, M.A., Ocal, C., Espinosa, J.C., Oesch, B., and Gasset, M. (2002) *J Mol Biol*. **319**, 527-540
6. Caughey, B., and Baron, G.S. (2006). *Nature* **443**, 803-810.
7. Steele, A.D., Emsley, J.G., Ozdinler, P.H., Lindquist, S., and Macklis, J.D. (2006) *Proc Natl Acad Sci U S A.* **103**, 3416-3421.
8. Liang, J., Pan, Y. , Zhang, D., Guo, C., Shi, Y., Wang, J., Chen, Y., Wang, X., Liu, J., Guo, X., Chen, Z., Qiao, T., and Fan, D. (2007) *FASEB J.* **21**, 2247-2256
9. Hölscher, C., Bach, U.C., and Dobberstein, B. (2001) *J. Biol. Chem.* **276**, 13388-13394
10. Kim, S.J., Rahbar, R., and Hegde, R.S. (2001) *J Biol Chem.* **276**, 26132-26140
11. Stewart, R.S., and Harris, D.A. (2003) *J Biol Chem.* **278**, 45960-45968
12. Hegde, R.S., and Rane, N.S. (2003) *Trends Neurosci.* **26**, 337-339.
13. Ma, J., and Lindquist, S. (2002) *Science* **298**, 1785-1788
14. Ma, J., Wollmann, R., and Lindquist, S. (2002) *Science* **298**, 1781-1785
15. Rane, N.S., Yonkovich, J.L.,and Hegde, R.S. (2004) *EMBO J.* **23**, 4550-5459
16. Ma, J., and Lindquist, S. (2001) *Proc Natl Acad Sci U S A.* **98,** 14955-14960
17. Yedidia, Y., Horonchik, L., Tzaban, S., Yanai, A., and Taraboulos A. (2001). *EMBO J.* **20**, 5383–5391.
18. Drisaldi, B., Stewart, R.S., Adles, C., Stewart, L.R., Quaglio, E., Biasini, E., Fioriti, L., Chiesa, R., and Harris, D.A.(2003) *J. Biol. Chem.* **278**, 21732-21743
19. Crozet, C., J. Vezilier, J., V. Delfieu,V., Nishimura,T., Onodera, T., Casanova, D., Lehmann, S., and Beranger, F.. (2006) *Mol Cell Neurosci.* **32**, 315-323.
20. Rambold, A.S., Miesbauer, M., Rapaport, D., Bartke, T., Baier, M., Winklhofer, K.F., and Tatzelt, J. (2006) *Mol Biol Cell.* **17**, 3356-3368
21. Wang, X., Wang, F., Arterburn, L., Wollmann, R., and Ma, J. (2006) *J Biol Chem.* **281**, 13559-13565
22. Roucou, X., Guo, Q., Zhang, Y., Goodyer, C.G., and LeBlanc, A.C. (2003) *J. Biol. Chem.* **278**, 40877-40881.
23. Orsi, A., Fioriti, L., Chiesa, R., and Sitia, R.(2006) *J. Biol. Chem.* **281**, 30431-30438
24. Hegde, R.S., and Lingappa, V.R. (1996) *Cell.* **85**, 217-228
25. Schägger, H. (2006) *Nature Protocols* **1**, 16-22
26 **O**tt C.M., and Lingappa V.R. (2004) *Biochemistry* **43**, 11973-82
27 Lorenz, H., Windl, O., and Kretzschmar, H.A. (2002) *J. Biol. Chem.* **277**, 8508–8516
28. Hosokawa, T., Tsuchiya, K., Sato, I., Takeyama, N., Ueda, S., Tagawa, Y., Kimura, K.M., Nakamura, I., Wu, G., Sakudo, A., Casalone, C., Mazza, M., Caramelli, M., Takahashi, H., Sata, T., Sugiura, K., Baj, A., Toniolo, A., and Onodera, T. (2008) *Biochem Biophys Res Commun.* **366**, 657-663.
29. Say, I.H., and Hooper, N.M. (2007) *Proteomics* **7**, 1059-1564.
30. Levine, C.G., Mitra, D., Sharma, A., Smith, C.L., and Hegde, R.S. (2005) *Mol Biol Cell.* **16**, 279-291
31. Touriol, C., Bornes, S., Bonnal, S., Audigier, S., Prats, H., Prats, A.C., and Vagner, S. (2003) *Biol. Cell.* **95**, 169-178
32 Sasaki, A., Inagaki-Ohara, K., Yoshida, T., Yamanaka, A., Sasaki, M., Yasukawa, H., AKoromilas, A.E., and Yoshimura, A. (2003) *J Biol Chem.* **278**, 2432-3246
33. Sorensen, V., Nilsen, T., and Wiedlocha, A.. (2006) *Bioessays* **28**, 504-514
34. Rogers, G.W. Jr, Edelman, G.M., and Mauro, V.P. (2004) *Proc Natl Acad Sci U S A.* **101**, 2794-2799.
35.Mironov, A. Jr, D. Latawiec, D., Wille, H., Bouzamondo-Bernstein, E., Legname, G., Williamson, R.A., Burton, D., DeArmond, S.J., Prusiner, S.B., and Peters, P.. (2003) *J. Neuroscience* **23**, 7183-7193
36. Mehdi, H., Ono, E., and Gupta, K.C.(1990) *Gene*. **91**, 173-178
37.Chang, K.J., Lin, G., Men, L.C., and Wang, C.C. (2006) *J Biol Chem.* **281**, 7775-7783
38. Derrington, E., Gabus, C., Leblanc, P., Chnaidermann, J., Grave, L., Dormont, D., Swietnicki, W., Morillas, M., Marck, D., Nandi, P., and Darlix, J.L. (2002) *C R Biol.* **325**,17-23
39. Geiss-Friedlander R., and F. Melchior. (2007) *Nat. Rev. Mol. Cell. Biol.* **8**, 947-956.
40. Ghaemmaghami S, Phuan PW, Perkins B, Ullman J, May BC, Cohen FE, Prusiner SB (2007) *Proc Natl Acad Sci U S A.* **104**,17971-6.

ACKNOWLEDGMENTS

We thank C. Albo and M. Seisdedos for their technical support. A. Bernad, D. Harris, R.S. Hegde, C. Korth, J. Fominaya and S. Saghafi are acknowledged for sharing reagents and for their helpful comments. Funding was provided by grants SAF2006-00418 (MG) and FIS PI050912 (MC) from the Ministerio de Ciencia e Innovación (MG) and FOOD-CT-2004 506579 (MG) from the EU.

Keywords: alternative translation initiation, cellular prion protein, protein isoforms, protein multiplicity

The abbreviations used are: PrP, prion protein, PrP^{C}, cellular prion protein, PrP(M15), isoform produced by translation starting at M15; PrP(M8), isoform produced by translation starting at M8; PIPLC, phosphatidylinositol-specific phospholipase C; Ha, syrian hamster, Mo, mouse, Hu, human, Bo, bovine, Ov, ovine, Mi, mink, Ra, rabbit, Ho, horse.

FIGURE LEGENDS

Figure 1. **Alternative translation start sites in the PrP mRNA signal sequence coding region. (A)** Classification of PrP signal sequence based on the presence of Met residues at the h-region boundaries. **(B)** Potential translation start sites in the HaPrP signal sequence mRNA coding region. AUG (thick) and non-AUG (thin) triplets are underlined. Arrows indicate the positions of insertions used for reading frame shifts in the generation of the 11C12, 13G14 and 16C17 mutants.

Figure 2. Translated forms from PrP mRNA. (A) *In vitro* translation of the mRNA of HaPrP wt and HuPrP wt and of their signal sequence mutants. **(B)** Cell-free synthesis of HaPrP wt, HaPrP(M1S), HaPrP(M1SM15S), HuPrP wt and HuPrP(M1S). The HuPrP(M1SM8S) and HaPrP(M1SM15S) mutants behaved similarly. Each of the mRNAs was translated in the rabbit reticulocyte lysate translation system in the presence of pancreatic microsomes and then immunoprecipitated with 3F4 mAb. The immunoprecipitated products were divided into two aliquots, one of which was digested with PNGase F as indicated. Relative sample loads are indicated at the bottom of the lanes. **(C)** Accessibility of the translation-translocation products of HaPrP wt, HuPrP wt and of their M1S mutants to externally added proteases in the total reaction mixtures (left) and in their sealed membrane fractions (SM, right). Each of the mRNAs was translated in the rabbit reticulocyte lysate translation system in the presence of pancreatic microsomes and then divided in three aliquots: i) untreated, ii) digested with proteinase K, and iii) digested with proteinase K in the presence of 0.5% Triton X-100 as a control for full accessibility. For SM analysis, HaPrP(M1S) was loaded in a 10x excess compared to HaPrP wt.

Figure 3. Expression of HaPrP(M15) in CHO cells. (A) Transient expression of HaPrP wt and of its mutants in CHO cells. After 48 h of co-transfection with pEYFP, cells were harvested, lysed and immunoblotted with antibodies against PrP (3F4), YFP and β-actin, respectively. Similar results were obtained using COS-7 cells. (**B**) Comparison of HaPrP(M1S) with 1-254, 15-254, 15-231 and 23-231 PrP chains produced in *E.coli* inclusion bodies by western blot. The Tris-Tricine SDS-PAGE was performed using 16.5% gels and the blot was probed with 3F4.

The migration of the recombinant PrP(15-254) chain is depicted with a straight line **(C)** Enzymatic deglycosylation with PNGase F of HaPrP wt and of its M1S mutant. **(D)** Incorporation of HaPrP wt and of its M1S and Δ14 mutants into cytosolic insoluble aggregates upon proteasome inhibition. After transfection (30 h), cells were treated in the absence of presence of 5μM MG132. Incubation with MG132 was either allowed to proceed for (+24) 24 h (irreversible inhibition) or (+4) after 4 h the media was replaced with MG132-free media and the incubation was continued for other 16 h (transient inhibition). Insoluble cytosolic aggregates were isolated as described in the method section.

Figure 4. Subcellular location of HaPrP(M15) in CHO cells. (A) Indirect immunofluorescence of CHO cells transiently transfected with HaPrP(Δ14). Fixed and permeabilized cells were stained with antibodies against PrP (3F4, red) and PDI (ER marker, green), and with the nuclear dye Hoescht (blue). The white bar represents 40 μm. **(B)** Partitioning of PrP between the nuclear (N) and the post-nuclear (PNS) fractions of transiently transfected CHO cells with HaPrP wt and its mutants. The displayed immunoblots were probed with α–PrP (3F4 and α-SP), α-Histone H3 (nuclear marker, around 17 kDa), and α-PDI (ER marker, around 60 kDa) antibodies.

Figure 5. Analysis of the nuclear PrP isoform in normal brain homogenates. (**A**) Removal of raft-bound PrP species from purified nuclei. Nuclei purified from hamster brain homogenates were digested with PIPLC and then centrifuged to remove GPI-bound co-purifying proteins. PIPLC-treated nuclei were then digested in the absence and presence of PNGase F. The blot was probed with 3F4. **(B)** PrP forms in PIPLC-treated nuclei from human cortex as detected by 3F4 and SP immunoreactivity. Samples a, b and c correspond to PIPLC-treated nuclear fractions purified from control human cortex homogenates. **(C)** Analysis of the covalent modifications of the nuclear PrP isoform. Denatured extracts of nuclei prepared from hamster brain were immunoprecipitated with 3F4 α-PrP. Lanes containing similar loads were probed with the following antibodies: mouse Trueblot (α-Mo), 3F4 α-PrP, α-SUMO1, α-ubiquitin (α-UB).

Figure 6. **HaPrP(M15) expression interferes with cell growth. (A)** Effect of the expression of HaPrP wt and its mutants on CHO and COS7 cell proliferation measured by BrdU incorporation. Data are shown as the mean ± s.d of three independent experiments, each performed in triplicate. Data were compared by one-way ANOVA with Bonferroni´s post-test analysis using GraphPad Prism v 4.0. Statistically significant differences between groups are indicated (* $p < 0.05$, ** $p < 0.01$, *** $p < 0.001$). **(B)** Typical cell cycle profile of YFP-selected CHO cells co-transfected with HaPrP wt and its mutants. YFP-expressing cells, separated by cell sorting, were stained with propidium iodide and analyzed by flow cytometry. **(C)** Cell cycle phase distribution of YFP-selected CHO cells expressing HaPrP wt and its mutants. Data are shown as the mean ± s.d of two independent experiments performed in duplicate. Data were compared by two-way ANOVA with Bonferroni´s post-test analysis using GraphPad Prism v 4.0. Statistically significant differences between groups are indicated (*** $p < 0.001$). For both panels, A and B, the relative expression level of the different construct was similar to that displayed in Figure 3A.

Table 1. HaPrP and HuPrP constructs

The HaPrP ORF, cloned into pcDNA4.1 under BglII/EcoRI targets, and the HuPrP ORF, cloned into pcDNA3.1 under BamHI/EcoRI targets, were used as templates for the generation of point, reading shift and deletion mutants using standard molecular biology protocols.

Name	Mutation	Forward oligo
HaPrPwt		
HaPrP(M1S)	ATG-1-TTC	5´ -GATCTACCTTCGCGAACCTTAGC
HaPrP(M15S)	ATG-15-TTC	5´-CTCTTTGTGGCTTTCTGGACTGATGTTGG
HaPrP(M1S,M15S)	ATG-1-TTC ATG-15-TTC	5´ -CTCTTTGTGGCTTTCTGGACTGATGTTGG 5´ -CTCTTTGTGGCTTTCTGGACTGATGTTGG
HaPrP(11C12)	+1 shift downstream codon 11	5´-CTGCTGGCACTCCTTTGTGGCTATGTG
HaPrP(13G14)	+1 shift downtream condon 13	5´-GGCACTCTTTGTGGGCTATGTGGACTGATG
HaPrP(16C17)	+1 shift downtream codon 16	5´-GTGGCTATGTGGCACTGATGTTGGC
HaPrP(Δ14)	Deletion of the 1-14 region	5´-CTGCTGGCACTCAGATCTATGTGGACTGAT
HuPrP wt		
HuPrP(M1S)	ATG-1-TTC	5´-GGTACCGAGTTCGGATCCGTCATTTTG
HuPrP(M8S)	ATG-8-TTC	5´-CTTGGCTGCTGGTTCCTGGTTCTCTTTG
HuPrP(M1S,M8S)	ATG-1-TTC ATG-8-TTC	5´-GGTACCGAGTTCGGATCCGTCATTTTG 5´-CTTGGCTGCTGGTTCCTGGTTCTCTTTG
HuPrP(5C6)	+1 shift downstream codon 5	5´-GCGAACCTTGGCCTGCTGGATGCTGG
HuPrP(11C12)	+1 shift downstream codon 11	5´-GCTGGATGCTGGTTCTCCTTTGTGGCCACATGG
HuPrP(13C14)	+1 shift downstream codon 13	5´-CTGGTTCTCTTTGTGCGCCACATG
HuPrP(16C17)	+1 shift downstream codon 16	5´-GTGGCCACATGGCAGTGACCTGGGC

Figure 1; Juanes et al.

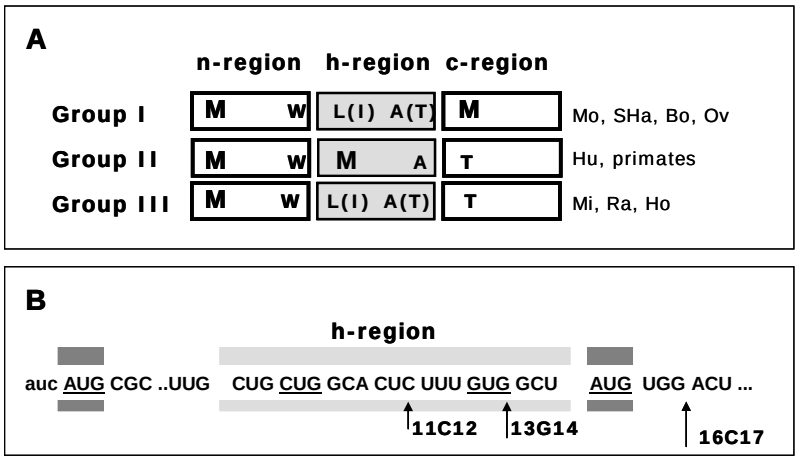

Figure 2; Juanes et al.

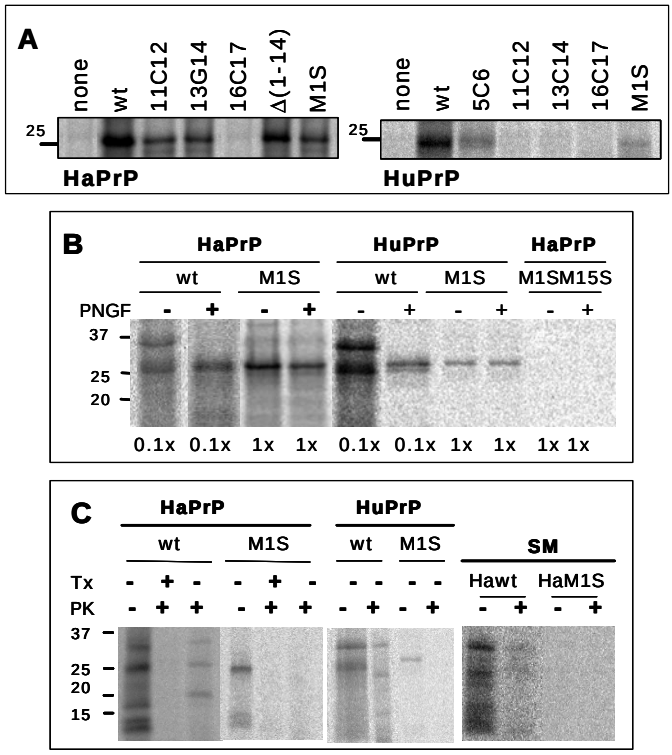

Figure 3, Juanes et al.

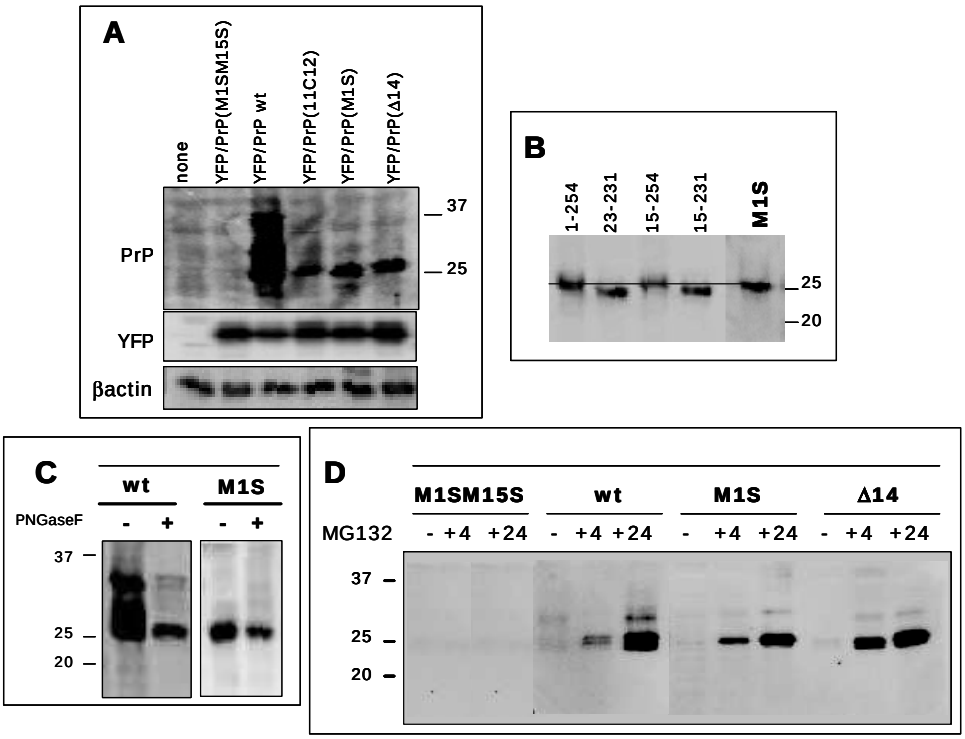

Figure 4; Juanes et al.

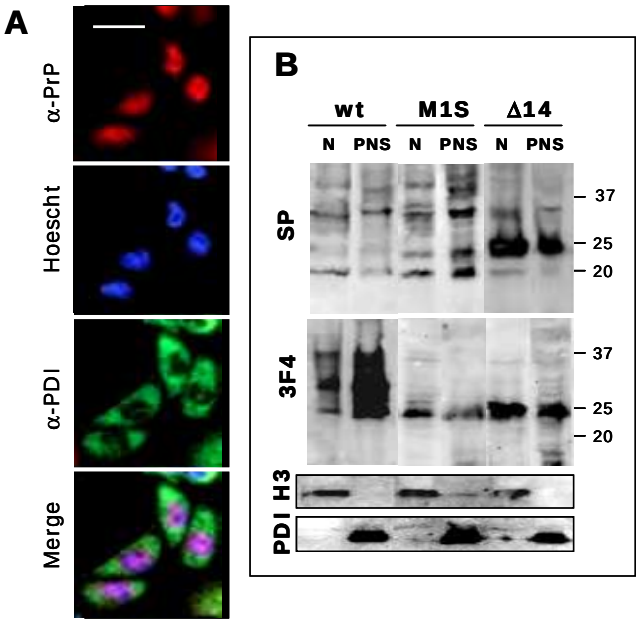

Figure 5; Juanes et al.

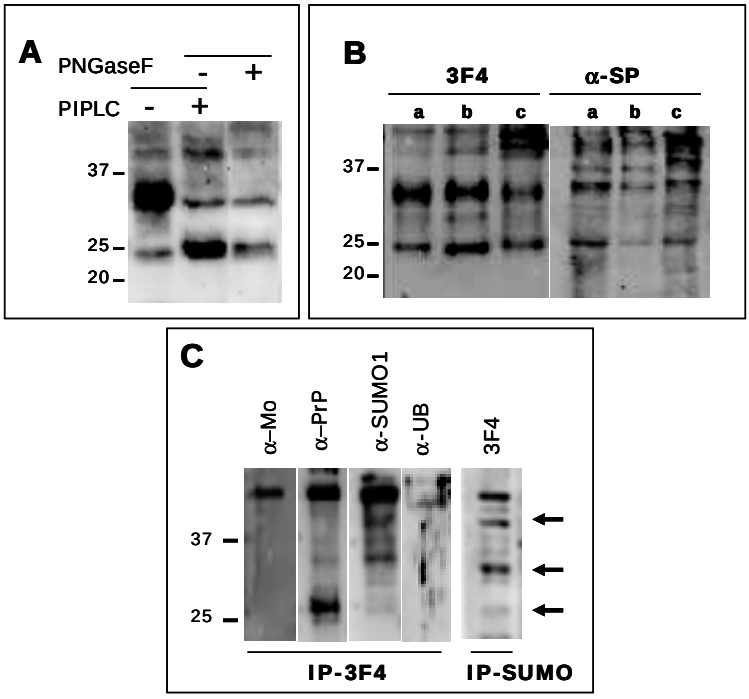

Figure 6; Juanes et al.